Carbohydrate Polymers 291 (2022) 119540

Contents lists available at ScienceDirect

Carbohydrate Polymers

journal homepage: www.elsevier.com/locate/carbpol

Periodate oxidation of plant polysaccharides provides polysaccharide-specific oligosaccharides

Carolina O. Pandeirada [a], Max Achterweust [a], Hans-Gerd Janssen [b,c], Yvonne Westphal [b], Henk A. Schols [a,*]

[a] Wageningen University & Research, Laboratory of Food Chemistry, Bornse Weilanden 9, 6708 WG Wageningen, the Netherlands
[b] Unilever Foods Innovation Centre – Hive, Bronland 14, 6708 WH Wageningen, the Netherlands
[c] Wageningen University & Research, Laboratory of Organic Chemistry, P.O. Box 8026, 6700 EG Wageningen, the Netherlands

ARTICLE INFO

Keywords:
Periodate oxidation
Plant polysaccharides
Depolymerization
Oxidized oligosaccharide clusters

ABSTRACT

Although polysaccharides are frequently used in foods, detailed characterization and/or identification of their structures using a single method remains a challenge. We investigated the suitability of periodate oxidation as an approach to depolymerize polysaccharides, allowing characterization and/or identification of the original polysaccharides based on ESI-MS analyses of the released oligosaccharides. Various periodate oxidation conditions were tested on (arabino)xylan, galactomannan, xyloglucan and homogalacturonan. Each polysaccharide required a different oxidation condition to release a substantial level of oligosaccharides. These oligosaccharides had highly complex structures due to the presence of e.g., dialdehyde sugars, hemialdals, and remnants of (oxidized) sugars, as verified by ESI-MS/MS. Despite these oligosaccharides were highly complex and lost some polysaccharide structural features, each periodate-oxidized sample comprised polysaccharide structure-dependent MS oxidized oligosaccharide profiles. Our findings are a good starting point to find a more generic chemical polysaccharide depolymerization approach based on periodate oxidation to identify polysaccharides by oligosaccharides fingerprinting using MS.

1. Introduction

Plant polysaccharides are the most abundant biomacromolecules in nature and abundantly present in foods (Harris & Smith, 2006; Saha et al., 2017). Plant polysaccharides have also been explored as food additives to modulate the functional properties of foods (Harris & Smith, 2006). Although polysaccharides are widely used in food products and involved in a wide variety of functional properties, detailed characterization of their structures remains a challenge.

Characterization of polysaccharides is laborious and often requires the combined use of multiple techniques. Gas chromatography (GC), liquid chromatography (LC) or nuclear magnetic resonance (NMR) spectroscopy can be used to determine the sugar composition after acid hydrolysis (De Ruiter et al., 1992; De Souza et al., 2013; Peterson, 1974; Ruiz-Matute et al., 2011; Willför et al., 2009). The type of glycosidic linkages can be studied by NMR or permethylation analysis (Sims et al., 2018). Non-sugar substitution, such as the presence of methyl-esters, acetyl- and hydroxycinnamoyl groups can be assessed through alkaline hydrolysis with GC and high-performance (HP)LC analysis (Beaugrand et al., 2004; Huisman et al., 2004). All these methods are complex and laborious and hence, there remains a need for a more rapid method to characterize and/or identify polysaccharide structures.

Enzymatic depolymerization of polysaccharides into structure-informative (diagnostic) oligosaccharides followed by separation,

Abbreviations: AX, arabinoxylan; BWX, birch wood xylan; DO, degree of oxidation; DP, degree of polymerization; ESI-MS, electonspray ionization - mass spectrometry; GC, gas chromatography; GM, galactomannan; $HexA^{m}_{n}$, oligomer composed of *n* GalA units and *m* methyl-esters; HG, homogalacturonan; H_mP_n, oligomer composed of *m* hexoses and *n* pentoses; H_n and H'_n, hexose oligomer and oligomer with*n*dialdehyde hexoses; HPAEC-PAD, high-performance anion-exchange chromatography with pulsed amperometric detection; HPSEC-RI, high performance size exclusion chromatography with refractive index detection; IO_4, periodate; Mw, molecular weight; NMR, nuclear magnetic resonance; (N)RE, (non-)reducing end; ox-DP_n, DP-clusters of oxidized oligosaccharides; P_n andP'_n, pentose oligomer and oligomer with*n*dialdehyde pentoses; pOx-PS, periodate-oxidized polysaccharide (AX, BWX, GM, XG, or HG); PS, polysaccharide; RT, room temperature; UA, uronic acids; (UHP)LC, (ultra-high-performance) liquid chromatography; XG, xyloglucan.

* Corresponding author.
E-mail address: henk.schols@wur.nl (H.A. Schols).

https://doi.org/10.1016/j.carbpol.2022.119540
Received 17 February 2022; Received in revised form 14 April 2022; Accepted 23 April 2022
Available online 27 April 2022

quantification and characterization of the released oligosaccharides allows a detailed characterization of polysaccharides (Bauer, 2012; Jermendi et al., 2022; Westphal et al., 2010). Although enzymatic digestion is a very powerful strategy to obtain diagnostic oligosaccharides, there is not a universal enzyme able to release oligosaccharides from all polysaccharides. All enzymes are highly polysaccharide-specific. Moreover they are sometimes limited in their action to degrade highly substituted polysaccharides (Lombard et al., 2014).

Periodate (IO_4^-) oxidation of polysaccharides has long been used for structural analysis of polysaccharides in combination with reduction of the periodate-oxidized polysaccharide followed by mild acid-hydrolysis [i.e., Smith degradation approach (Abdel-Akher et al., 1952; Aspinall & Ross, 1963; Simas-Tosin et al., 2013)]. Periodate oxidation is a well-known reaction that leads to specific oxidation of free vicinal hydroxyl groups to aldehydes with internal ring cleavage (Kristiansen et al., 2010), creating polyaldehydes. For the reaction to take place, vicinal hydroxyl groups must be oriented in an equatorial (*eq.*)-*eq.* or axial (*ax.*)-*eq.* positions. The periodate oxidation reaction is mostly performed in aqueous systems; however, in such systems, the aldehyde groups of periodate-oxidized polysaccharides can react with hydroxyl groups, forming inter- and/or intra-hemiacetal bonds, or with water, forming hemialdals or hydrated aldehydes (da Silva et al., 2020; Nypelö et al., 2021; Sirviö et al., 2014; Spedding, 1960). These aldehyde side oxidation reactions might form very complex saccharide chemical structures, complicating the analysis of the resulting periodate-oxidized saccharides and consequent characterization of the respective native polysaccharide structure. For detailed mechanistic insights about periodate oxidation, the reader is referred to the works of Abdel-Akher et al. (1952), Bobbitt (1956), Hough et al. (1958), Perlin (2006), and Kristiansen et al. (2010).

Periodate oxidation of polysaccharides can also lead to depolymerization of polysaccharides, which depends on the concentration of $NaIO_4$ (Chemin et al., 2016; Ding et al., 2017), temperature (Gupta et al., 2013; Kholiya et al., 2016), time (Kochumalayil, Zhou, Kasai, & Berglund, 2013), and pH (Kholiya et al., 2016). Thus, despite aldehyde side oxidation reactions might occur, given the high specificity of $NaIO_4$ to oxidize vicinal diols and considering that periodate oxidation can lead to polysaccharide depolymerization, periodate oxidation of polysaccharides might initiate the formation of diagnostic oligosaccharides in a faster and more generic manner than by using enzymes. For example, periodate oxidation of (arabino)xylans allows to determine branching points because the (1→4)-linked xylose (Xyl) residues in the polymer backbone that are 2-*O*- and/or 3-*O*-substituted cannot be oxidized due to absence of vicinal diols (Aspinall & Ross, 1963). Although scarce, few studies have made use of electrospray ionization (ESI-)MS to study the structure of oligosaccharides obtained after derivatization and/or hydrolysis of periodate-oxidized (poly)saccharides (Majee et al., 2016; Morelle et al., 1998; Pereira et al., 2018; Simões et al., 2016). Nonetheless, to the best of our knowledge, there are no studies reporting the use of ESI-MS to characterize oligosaccharides directly obtained from periodate oxidation of polysaccharides. Thus, our study aimed to investigate if periodate oxidation of plant polysaccharides leads to the formation of oligosaccharides that allow characterization and/or identification of polysaccharides using ESI-MS. To do this, various periodate oxidation conditions ($NaIO_4$ concentration, temperature, and time) were tested on five plant polysaccharides (arabinoxylan, xylan, galactomannan, xyloglucan, and homogalacturonan), and the resulting periodate-oxidized polysaccharide products were characterized.

2. Materials and methods

2.1. Materials

Wheat arabinoxylan (AX) of medium viscosity was obtained from Megazyme (arabinose (Ara):Xyl = 38:62, Purity > 95%, Wicklow, Ireland), birch wood xylan (BWX) from Sigma (Darmstadt, Germany), guar galactomannan (GM; mannose (Man): galactose (Gal) = 2:1) was from BFGoodrich Diamalt GmbH (Munich, Germany), tamarind seed xyloglucan (XG) from Dainippon Sumitomo Pharma Co. Ltd., (Osaka, Japan), and lemon homogalacturonan (HG) with a high degree of methyl-esterification was provided by Copenhagen Pectin A/S (Lille Skensved, Denmark). Sodium metaperiodate ($NaIO_4$, 98%) was purchased from Alfa Aesar (Thermo Fisher, Kandel, Germany). Ethylene glycol was from Merck (Darmstadt). Methanol, formic acid, and LC-MS water used in MS experiments were of ultra (U)HPLC-grade (Biosolve, Valkenswaard, The Netherlands). All water was purified in a Milli-Q system from Millipore (Molsheim, France), unless otherwise mentioned.

2.2. Periodate oxidation of polysaccharides

Wheat AX, BWX, GM, XG, and HG were periodate oxidized using various ratios of μmol $NaIO_4$/mg polysaccharide (PS) with two reaction temperatures (room temperature – RT, and 70 °C), and two reaction times (6 and 24 h). The $NaIO_4$/PS ratios tested were 3.0, 6.0, and 12.0 μmol $NaIO_4$/mg PS, which should lead to approx. 50%, 100% and >100% oxidation of all investigated polysaccharides, respectively, except for HG. HG is expected to be fully oxidized already at 3.0 $NaIO_4$/PS ratio (Table 1). Here, we define 100% oxidation as oxidation of all sugar units containing free vicinal hydroxyl groups by $NaIO_4$ with formation of dialdehydes. To calculate these values, we assume that 1 mol of sugar unit containing vicinal diols (unsubstituted Xyl and all Ara units of AX and BWX; all Man units of GM; glucose (Glc) and substituted Xyl units of XG; and all galacturonic acid (GalA) units of HG) would consume 1 mol of $NaIO_4$, and that 1 mol of sugar unit containing three vicinal hydroxyl groups (Gal units of GM; and unsubstituted Xyl and Gal units of XG) would consume 2 mol of $NaIO_4$. The apparent molecular weight (Mw) of the polysaccharides investigated in this study and the theoretical amount of $NaIO_4$ (μmol) needed per mg of PS to have full oxidation is summarized in Table 1.

Periodate oxidation of plant polysaccharides was performed adapting the procedure used by Åman and Bengtsson (1991) omitting the reduction and mild acid hydrolysis steps. Briefly, the reaction volume was set at 40 mL, and 200 mg of PS powder was used in all experiments. Polysaccharides were dissolved in water, and the pH of the samples' solution was measured, which was 3.5, 5.3, 6.2, 6.3, and 6.5 for HG, XG, GM, BWX, and AX, respectively. Subsequently, a freshly prepared 250 μmol/mL $NaIO_4$ solution was added to the PS solution to reach the desired μmol $NaIO_4$/mg PS ratio (2.4, 4.8, and 9.6 mL of 250 μmol/mL $NaIO_4$ solution to have a μmol $NaIO_4$/mg PS ratio of 3.0, 6.0, and 12.0, respectively). The glass reaction flask was protected from light by covering the flask with aluminium foil, and the reaction was carried out for 6 or 24 h at RT under magnetic stirring or at 70 °C in an incubator under shaking. The reaction was quenched by adding 1.6 mL ethylene glycol, and the reaction mixture was dialysed (cut-off for globular

Table 1
Apparent molecular weight (Mw) of the polysaccharides investigated and theoretical amount of $NaIO_4$ (μmol) per mg of PS needed to have full oxidation of arabinoxylan (AX), birch wood xylan (BWX), galactomannan (GM), xyloglucan (XG), and homogalacturonan (HG).

Polysaccharides	Mw (kDa)	Theoretical amount of $NaIO_4$/PS needed (μmol $NaIO_4$/mg PS)
AX	350[a]	6.3
BWX	300[a] (pop. 1) 37[a] (pop. 2)	5.6
GM	1010[a]	6.1
XG	780[a]	6.8
HG	120[b]	3.1

pop. – population.
[a] Mw determined by HPSEC-RI using pullulan standards.
[b] Mw determined by HPSEC-RI using pectin standards.

proteins: 12–14 kDa, Medicell Membranes Ltd., London) against distilled water. The retentate was freeze-dried, yielding the final periodate-oxidized PS sample, named pOx-PS.

2.3. Sugar composition analysis by HPAEC-PAD

Sugar composition of (pOx-)AX, BWX, and HG was determined after methanolysis (2.0 M HCl in dried methanol, 16 h, 80 °C) and TFA acid hydrolysis (2.0 M, 1 h, 121 °C) as described elsewhere (Pandeirada et al., 2021). Hydrolysates were diluted in water to ±25 μg/mL before analysis. Sugar composition of (pOx-)GM and XG samples was accessed after pre-hydrolysis for 15 min at 30 °C in 72% (*w*/w) H_2SO_4 followed by hydrolysis for 3 h at 100 °C in 1.0 M H_2SO_4. Sulphuric acid hydrolysates were 100 times diluted with water before analysis. Monosaccharides released were analysed by High-Performance Anion-Exchange Chromatography with Pulsed Amperometric Detection (HPAEC-PAD). An ICS-5000 HPLC system (Dionex, Sunnyvale, CA, USA) equipped with a CarboPac PA1 guard column (2 mm ID × 50 mm) and a CarboPac PA-1 column (2 mm × 250 mm; both from Dionex) was used for this analysis. Detection of the eluted compounds was performed by an ED40 EC-detector (Dionex) running in the PAD mode. Ten microliters of the diluted hydrolysates was injected on the system and compounds were eluted as described by Pandeirada et al. (2021). All samples were analysed in duplicate. Monosaccharide standards in a concentration range of 1.0–150 μg/mL were used for quantification. The collected data were analysed using Chromeleon 7.2 software (Dionex). The degree of oxidation (DO) (Eq. (1)) of samples was calculated based on the decrease in the sugar recovery relative to the respective native PS. The relative DO (DO_{Rel}) (Eq. (2)) was calculated using the theoretical maximum DO (DO_{Theo}) that each PS can reach and the calculated DO. DO_{Theo} was calculated based on the expected total remaining sugar content, i.e. all sugar units containing vicinal diols are oxidized and not detected as intact sugar anymore.

$$DO\ (\%, w/w) = 100 - Relative\ sugar\ recovery\ of\ pOx - PS \quad (1)$$

$$DO_{Rel}(\%, w/w) = \frac{DO}{DO_{Theo}} \times 100 \quad (2)$$

2.4. Uronic acid and methyl-ester content

The total uronic acid content of (pOx-)BWX and HG was determined using an automated colorimetric *m*-hydroxydiphenyl method (Blumenkrantz & Asboe-Hansen, 1973; Thibault & JF, 1979) after sulphuric acid-hydrolysis as described in Section 2.3.

For the determination of the methyl-ester content, (pOx-)HG samples were saponified at 5.0 mg/mL in 0.1 M NaOH for 24 h (1 h at 4 °C followed by 23 h at RT). The methanol released was quantified by gas chromatography (GC) using a method described elsewhere (Huisman et al., 2004). All analyses were performed in duplicate. The collected data were analysed using Xcalibur 4.1 software (Thermo Scientific).

2.5. Molecular weight distribution by HPSEC-RI

The average molecular weight (Mw) was determined by high performance size exclusion chromatography (HPSEC) on an Ultimate 3000 system (Dionex) coupled to Shodex RI-101 detector (Showa Denko K.K., Tokyo, Japan) as described by Pandeirada et al. (2021). Columns were calibrated with pullulan (0.180–708 kDa; Polymer Laboratories, UK) and pectin standards (10–100 kDa, as estimated by viscometry (Deckers et al., 1986)). Standards and samples were analysed at 1.0 mg/mL. Collected data were analysed using Chromeleon 7.2 software (Dionex).

2.6. Electrospray ionization mass spectrometry (ESI-MS) and tandem MS

ESI-MS and ESI-MS/MS experiments were carried out on an LTQ-VelosPro mass spectrometer (Thermo Scientific) equipped with a heated ESI probe. MS data were acquired in positive ion mode for pOx-AX, pOx-BWX, pOx-GM, and pOx-XG samples, which were diluted to 2.0 mg/mL in water and introduced into the electrospray source at 20 μL/min. Spectra were recorded for 2.5 min. Instrument settings were: source heater temperature 425 °C, capillary temperature 275 °C, sheath gas flow 30 units, source voltage 5.0 kV and *m/z* range 150–1500. The MS data for pOx-HG were obtained in negative ion mode using a sheath gas flow of 50 units, and a source voltage 3.5 kV, with the rest of the parameters being the same as described above. The pOx-HG samples were diluted to 2.0 mg/mL in methanol:water (1:1, *v*/v) containing 0.1% (*v*/v) formic acid and introduced into the electrospray source at 20 μL/min. MS/MS spectra of all samples were acquired by collision-induced dissociation (CID) using a collision energy set at 32%, with a minimum signal threshold of 500 counts at an activation Q of 0.25 and activation time of 10 ms were used. MS data were processed using Xcalibur 4.1 software (Thermo Scientific).

3. Results and discussion

Various plant polysaccharides, wheat arabinoxylan (AX), birch wood xylan (BWX), guar galactomannan (GM), tamarind seed xyloglucan (XG), and highly methyl-esterified lemon homogalacturonan (HG), were periodate-oxidized under various conditions. It was investigated whether periodate oxidation of plant polysaccharides could lead to the formation of oligosaccharides that allow structural characterization and/or identification of polysaccharides in a faster and more generic manner than by using enzymes. Two reaction temperatures (room temperature (RT) and 70 °C), two reaction times (6 and 24 h), and three different periodate-to-polysaccharide (PS) ratios were tested. The $NaIO_4$/PS ratios tested were 3.0, 6.0, and 12.0 μmol $NaIO_4$/mg PS, which theoretically lead to approx. 50%, 100% and ≫100% oxidation of all investigated polysaccharides, respectively, except for HG. HG is expected to be fully oxidized at 3.0 $NaIO_4$/PS ratio (Table 1).

3.1. Effect of periodate oxidation on the Mw distribution of polysaccharides

The influence of the various periodate oxidation conditions on the molecular weight (Mw) distribution of polysaccharides was studied by HPSEC. HPSEC profiles of all periodate-oxidized PS (pOx-PS) samples are shown in supplementary material (Fig. S1, AX and BWX; Fig. S2, GM and XG; and Fig. S3, HG). In general, all soluble pOx-PS samples had lower molecular weights than the respective native PS, in agreement with various studies (Chemin et al., 2016; Chetouani et al., 2017; da Silva et al., 2020; Gupta et al., 2013; Sirvio et al., 2011). All pOx-AX and pOx-BWX samples contained molecules within a degree of polymerization (DP) 2–20 (oligosaccharides) or larger. The extent of depolymerization of AX and BWX increased when the $NaIO_4$/PS ratio was raised from 3.0 to 12.0, in accordance with literature (Chemin et al., 2016), and the highest level of molecules comprising a DP 2–20 were obtained when the reaction was performed at RT for 6 h (Fig. 1A and B).

Regarding GM, XG, and HG samples, polysaccharide depolymerization releasing molecules within the DP 2–20 range mainly occurred when the reaction was performed at 70 °C for 24 h (Fig. 1C, D and E). Maximum GM and XG degradations were reached using a $NaIO_4$/PS ratio of 6.0 for 24 h at 70 °C. While for HG, maximum degradation was only obtained using a higher $NaIO_4$/PS ratio of 12.0 at 70 °C for 24 h. Most of the molecules in these samples contained a DP 2–20.

Overall, it can be stated that pentosans are more readily degraded by periodate than hexose- and hexuronic-based polymers. Oligosaccharides were obtained at any periodate oxidation condition for AX and BWX, whereas for GM, XG, and HG, a high level of oligosaccharides was only obtained at 70 °C using a $NaIO_4$/PS ratio ≥ 6.0 and a long reaction time of 24 h. These results show that periodate oxidation of plant polysaccharides can release oligosaccharides for all polysaccharides.

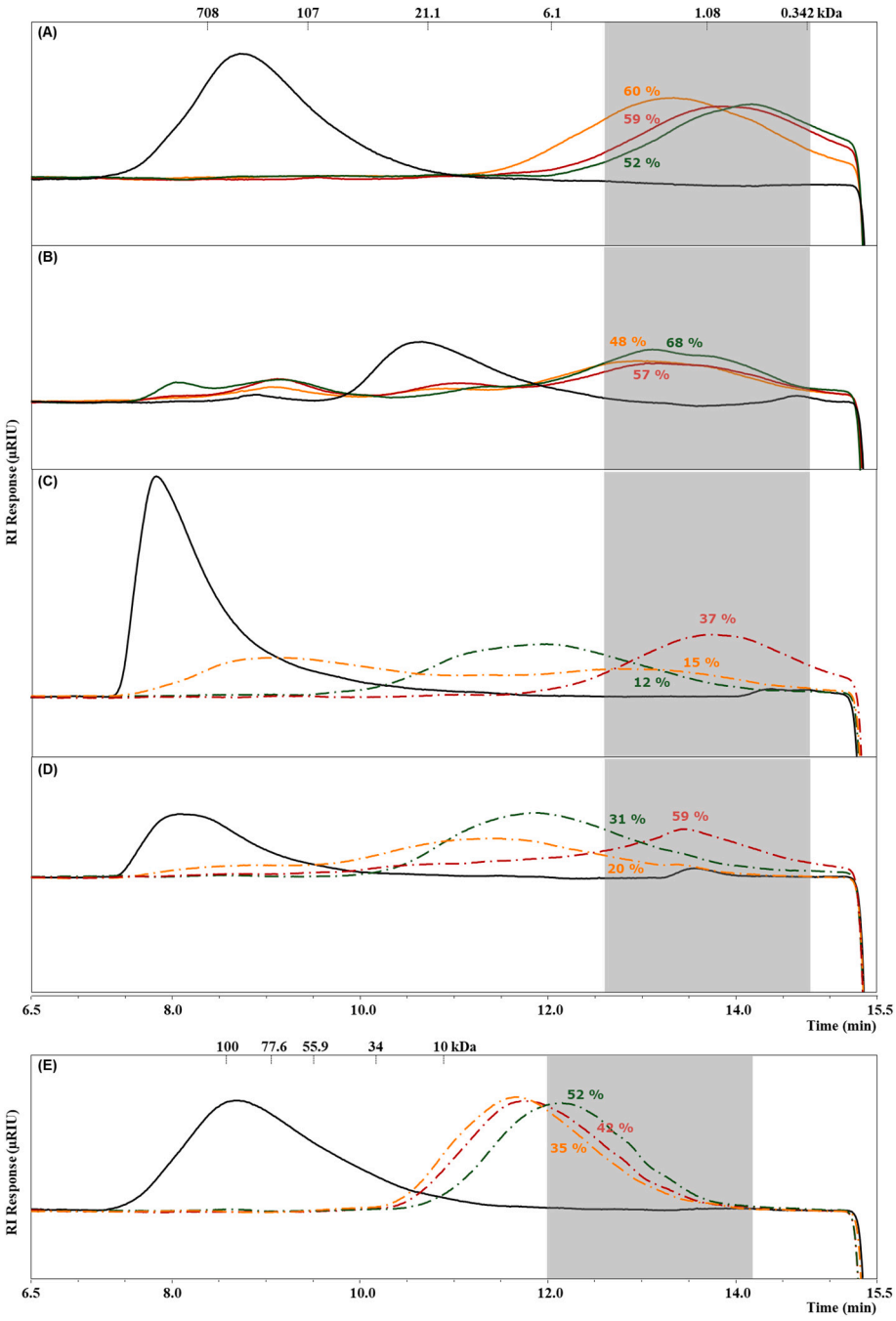

Fig. 1. HPSEC elution patterns of the periodate-oxidized AX (A) and BWX (B) samples at room temperature for 6 h, and of the GM (C), XG (D), and HG (E) samples oxidized at 70 °C for 24 h. Native PS samples are shown in black lines, and periodate-oxidized samples with 3.0, 6.0 and 12.0 $NaIO_4$/PS are shown in orange, red, and green lines, respectively. (—) 6 h reaction; (– · – · – · –) 24 h reaction. Pullulan and pectin standards were used to calibrate the system for neutral polysaccharides and HG, respectively. Grey boxes indicate the time range corresponding to an apparent DP between 2 and 20. Relative area percentages (%) of molecules within a DP 2–20 (grey box) present in the periodate-oxidized samples in comparison to the total area of the respective native sample are given in orange, red, and green for the reactions performed using 3.0, 6.0 and 12.0 $NaIO_4$/PS, respectively. (For interpretation of the references to colour in this figure legend, the reader is referred to the web version of this article.)

Formation rates depend on the conditions applied and differ per PS structure.

3.2. General composition of periodate-oxidized/degraded polysaccharides

To investigate the influence of the periodate oxidation conditions on the general composition of polysaccharides, the sugar composition of all (pOx-)PS samples, and the methyl-esterification content of pectin samples was investigated. The yield, sugar recovery, and degrees of oxidation (DO and DO_{Rel}) of all pOx-PS samples investigated in this study are shown in Table S1 and Fig. S4. In general, the sugar recovery of pOx-PS samples relatively to the respective native PS was lower than 75% (*w*/w), as expected due to the oxidation process. In the following paragraphs, a detailed description of the composition of the samples containing the highest levels of molecules in the DP 2–20 range (based on the HPSEC results, Section 3.1) is given and will be discussed to understand if the oligosaccharides released provide information on the native PS structure.

3.2.1. Arabino(xylan)

pOx-AX samples containing the highest level of molecules in the DP 2–20 range were obtained at RT and 6 h reaction time (Fig. 1A). For these samples, the decrease in the Ara and Xyl recoveries increased when the $NaIO_4$/PS ratio was increased from 3.0 to 12.0 (Fig. 2A). At a $NaIO_4$/PS ratio of 12.0 at RT and 6 h reaction time, no Ara was detected anymore (Fig. 2A), suggesting complete oxidation and/or degradation of the Ara side chains. At this condition, still 9.7% (*w*/w) Xyl was recovered. Retrieval of Xyl and disappearance of Ara at high $NaIO_4$ concentrations is expected because only unsubstituted Xyl units are susceptible to oxidation, whereas all Ara units can be oxidized.

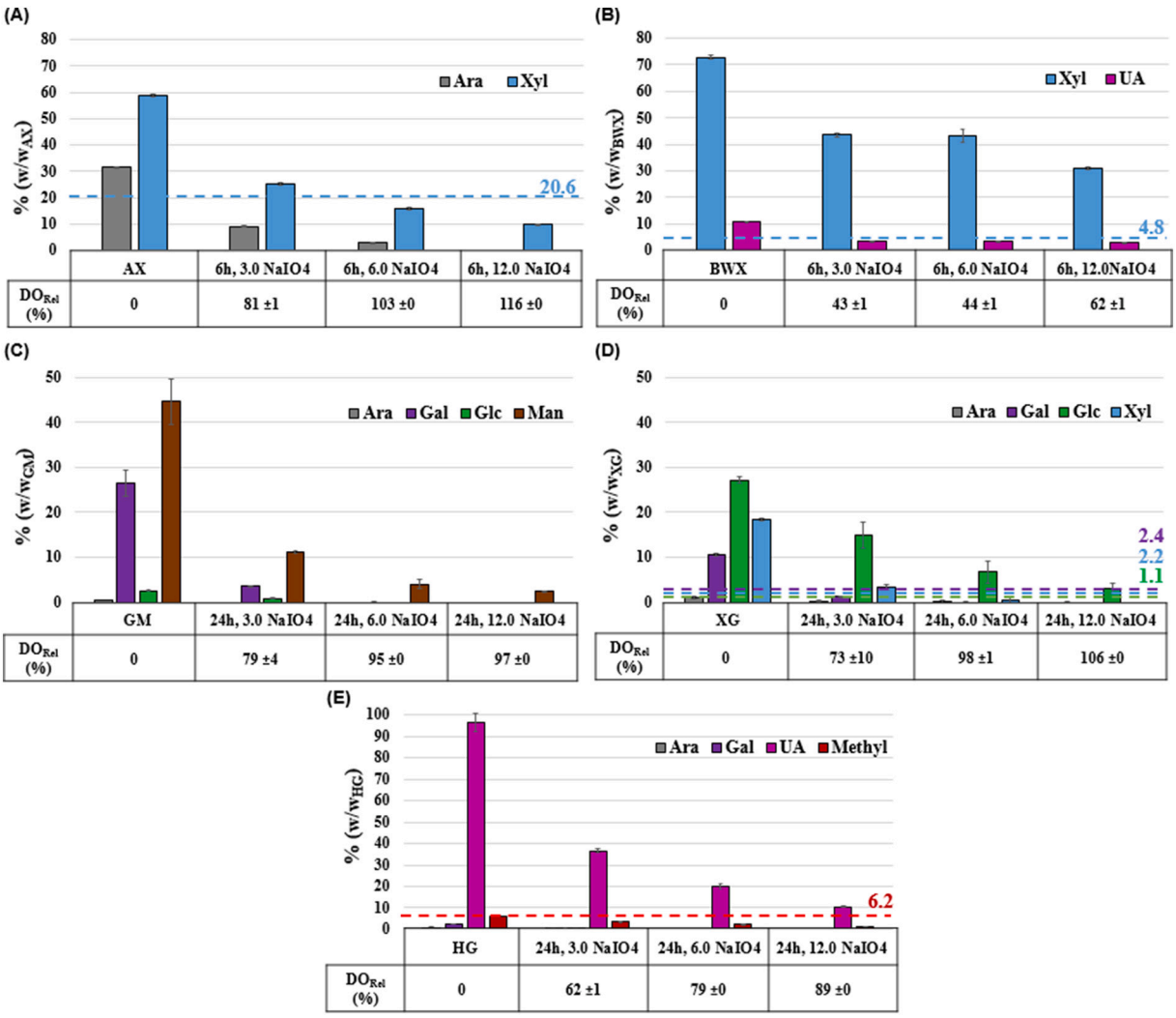

Fig. 2. Sugar recovery of the native and periodate-oxidized polysaccharide samples, AX (A) and BWX (B) at room temperature (RT) for 6 h, and of GM (C), XG (D), and HG (E) at 70 °C for 24 h, using a μmol $NaIO_4$/mg PS ratio of 3.0, 6.0 and 12.0. Uronic acid (UA) recovery of BWX and HG samples, and Methyl-ester recovery of HG samples are given. Coloured dashed lines (– – –) represent the theoretical minimum amount of sugar unit (blue, Xyl; purple, Gal; green, Glc) and methyl-ester (red) that are expected to be obtained at 100% oxidation. When no dashed line is depicted for a given sugar, it indicates that a minimum amount of 0 can be obtained. Relative degree of oxidation (DO_{Rel}) in % is given for each pOx-sample in the table inserted below each graph. DO_{Rel} for pOx-HG samples is based on the decrease in the UA recovery. (For interpretation of the references to colour in this figure legend, the reader is referred to the web version of this article.)

The Xyl recovery of 9.7% is lower than the theoretically value (~20.6%) that would be obtained if AX is 100% oxidized (Fig. 2A). This suggests that overoxidation of the pOx-AX at RT for 6 h using a $NaIO_4$/PS ratio of 12.0 occurred (DO_{Rel} > 100%). This might be due to oxidation and/or degradation of substituted Xyl units, which might have been caused by cleavage of the Ara side chains, leaving new unsubstituted Xyl units available for oxidation. All together this indicates that high $NaIO_4$ concentrations can lead to removal of the PS structural features, in that way hindering the formation of oligosaccharides that can be used for structural characterization of the original PS. Clearly, overoxidation of the polymers should be avoided.

At a $NaIO_4$/PS ratio of 6.0 for 6 h at RT, pOx-AX recovered minor amounts of Ara (<3.0%), and Xyl underwent only minor overoxidation and/or degradation (recovered Xyl just slightly below 20.6%), showing that this pOx-AX was almost completely oxidized (Fig. 2A). This indicates that for AX, the treatment at RT for 6 h using a $NaIO_4$/PS ratio of 6.0 might provide the highest level of structure-indicative oligosaccharides.

For BWX, the highest level of molecules in the DP 2–20 range was also obtained at RT and 6 h reaction time (Fig. 1B). The decrease in the Xyl and uronic acids (UA) recoveries of pOx-BWX at RT for 6 h was higher at a $NaIO_4$/PS ratio of 12.0 than at a $NaIO_4$/PS ratio of 3.0 or 6.0 (Fig. 2B). None of the former oxidation conditions led to complete BWX oxidation. This suggests that a moderately substituted xylan with UA (BWX) is more difficult to oxidize than a highly substituted xylan with Ara units (AX) at RT. This might be due to incomplete solubilization of BWX at RT, or due to easier formation of stable hemiacetal rings in a low substituted xylan, preventing oxidation of the Xyl residues, as suggested by Åman and Bengtsson (1991) and Izydorczyk and Biliaderis (1995). Yet, full oxidation of the BWX would completely modify the BWX structure and prevent the formation of diagnostic oligosaccharides. The pOx-BWX samples obtained at RT and 6 h treatment displayed a DO_{Rel} ranging from 43 to 62% at a $NaIO_4$/PS ratio of 3.0 and 12.0 (Fig. 2B), respectively, and are hence likely to contain BWX structure-informative oligosaccharides.

3.2.2. *Galactomannan and xyloglucan*

The pOx-GM and pOx-XG samples that displayed the highest level of molecules with a DP 2–20 were obtained using a $NaIO_4$/PS ratio of 6.0 for 24 h at 70 °C (Fig. 1C and D), a condition that theoretically leads to full oxidation of GM and XG (Table 1). Under this condition, pOx-GM and pOx-XG were obtained with a DO_{Rel} of 95 and 98% (Fig. 2C and

D), respectively. Minor amounts of Man and Glc (<7.0%) were recovered in these pOx-GM and pOx-XG samples, respectively. In GM and XG, all sugar units can be periodate-oxidized since all moieties contain vicinal diols. This indicates that in both the GM and XG samples, the sugar side chains were more readily oxidized and/or degraded than the backbone. This agrees with previous studies on periodate oxidation of GM and XG (da Silva et al., 2020; Gupta et al., 1987; Kochumalayil et al., 2013a; Kochumalayil et al., 2013b). Thus, if the sugar units in the side chains of GM and XG are oxidized without being removed from the (oxidized) polymer backbone, the released oligosaccharides from the pOx-GM and pOx-XG samples at a $NaIO_4$/PS ratio of 6.0 for 24 h at 70 °C might be diagnostic.

3.2.3. Homogalacturonan

The pOx-HG obtained using a $NaIO_4$/PS ratio of 12.0 at 70 °C for 24 h not only had the highest DO_{Rel} (89%, Fig. 2E), but it also had the highest level of molecules with a DP 2–20 (Fig. 1E). Although this pOx-HG comprised the highest level of oligosaccharides, it was also the pOx-

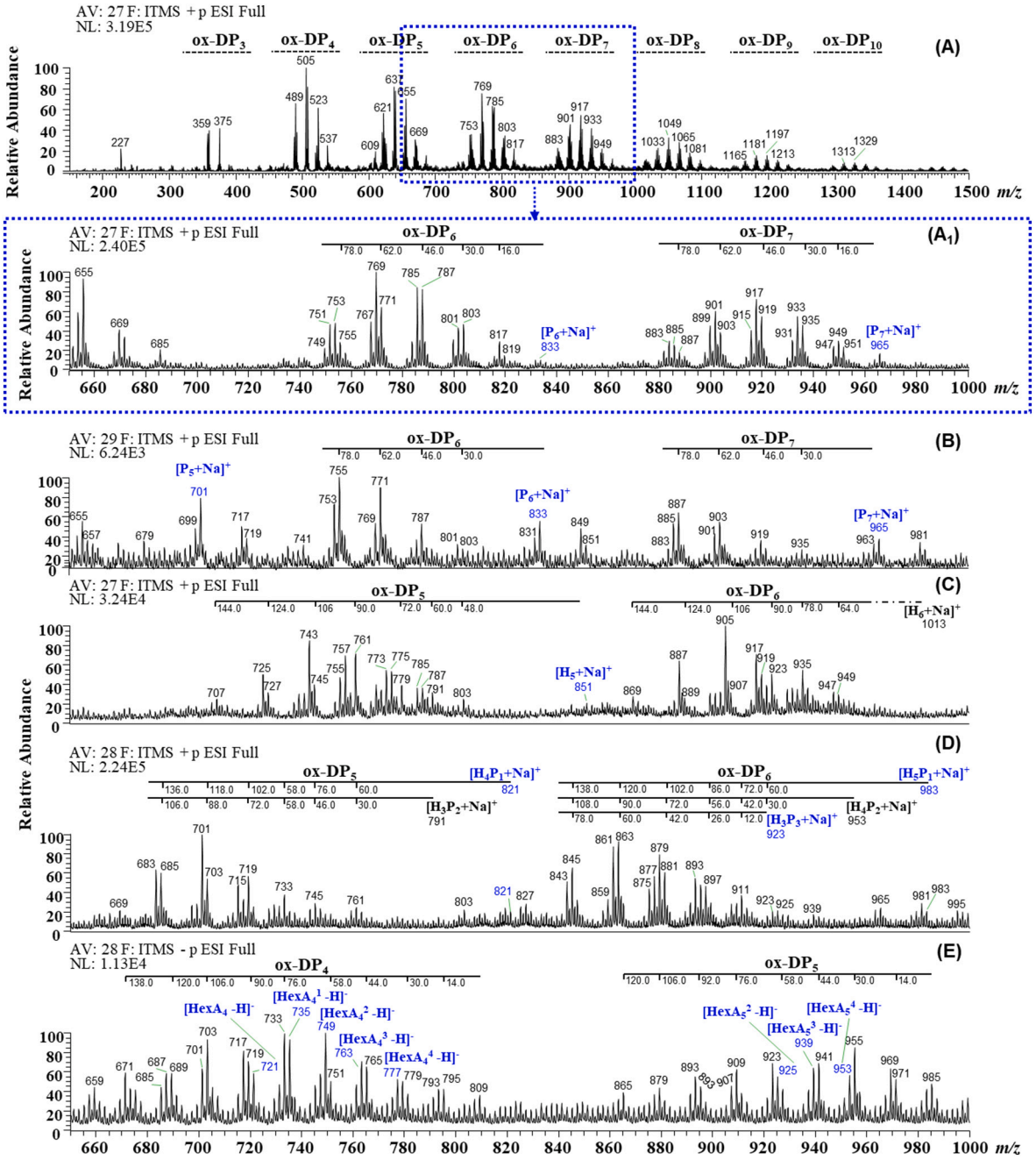

Fig. 3. Positive ion mode ESI mass spectrum of the periodate-oxidized (pOx-)AX (RT, 6 h, $NaIO_4$/PS of 6.0) (A), and a zoom-in of the *m/z* 650–1000 range of pOx-AX (RT, 6 h, $NaIO_4$/PS of 6.0) (A_1), pOx-BWX (RT, 6 h, $NaIO_4$/PS of 3.0) (B), pOx-GM (70 °C, 24 h, $NaIO_4$/PS of 6.0) (C), and pOx-XG (70 °C, 24 h, $NaIO_4$/PS of 6.0) (D). Negative ion mode ESI mass spectrum (*m/z* 650–1000) of the pOx-HG (70 °C, 24 h, $NaIO_4$/PS of 12.0) (E). $\mathbf{P_n}$ or $\mathbf{H_n}$ or $\mathbf{H_mP_n}$ – Oligomer composed of n pentoses (arabinose or xylose) or n hexoses (Gal or Man), or m hexoses (Gal or Glc) and n pentoses (xylose). $\mathbf{HexA^m_n}$ – Oligomer composed of n GalA units and m methyl-esters. $\mathbf{ox\text{-}DP_n}$ – *m/z* region of a cluster of oxidized oligosaccharides potentially with a n DP. *m/z* differences from each sub-oligosaccharide cluster with Δ −(x + n * 2) Da, with $n = 0$–4, to the corresponding non-oxidized DP-oligomer are depicted in (A_1–D). In (E), *m/z* differences from each sub-oligosaccharide cluster with Δ −(x + n * 2) Da, with n = 0–3, are given in relation the highest oxidized *m/z* value detect within each $\mathbf{ox\text{-}DP_n}$ cluster. Detected non-oxidized oligomers are highlighted in blue. (For interpretation of the references to colour in this figure legend, the reader is referred to the web version of this article.)

HG sample that had the lowest recovery of methyl-esters (22.3%, Fig. S5). The removal of methyl-esters indicates that the oligosaccharides obtained for pOx-HG at 70 °C for 24 h using a $NaIO_4$/PS ratio of 12.0 do not allow detailed characterization of the native HG structure. Although the other pOx-HG samples oxidized at RT, or at 70 °C for 6 h, recovered larger amounts of methyl-esters (72–88%, Fig. S5), they contained no or only minor levels of oligosaccharides (Fig. S3). Thus, although not fully diagnostic, the oligosaccharides present in pOx-HG (70 °C, 24 h, $NaIO_4$/PS ratio of 12.0) might still be useful to recognize an HG type structure.

3.3. ESI-MS analysis of (periodate-oxidized) oligosaccharides

To study the type of oligosaccharides formed upon periodate oxidation, samples containing oligosaccharides were analysed using electrospray ionization (ESI) mass spectrometry (MS) via direct infusion. The ESI-MS profiles (Fig. 3) obtained for each pOx-PS containing (diagnostic) oligosaccharides are shown and discussed below.

3.3.1. ESI-MS analysis of periodate-oxidized AX and BWX samples

HPSEC and compositional results indicated that pOx-AX at RT for 6 h using a $NaIO_4$/PS ratio of 6.0 likely had the highest level of diagnostic oligosaccharides. Hence, this sample was selected to be further analysed by ESI-MS. The selected pOx-AX mostly comprised oxidized oligosaccharides and a negligible level of pentose-oligomers (P_n; Fig. 3A), confirming the high DO of this sample. The released oxidized oligosaccharides had well-defined *m/z* regions, forming DP-clusters of oxidized oligosaccharides (identified as **ox-DP$_n$** in Fig. 3). These DP-clusters were composed of various sub-oligosaccharide clusters. To better visualize these clusters (**ox-DP$_n$**), and their respective sub-oligosaccharide clusters, a zoom-in of the *m/z* 650–1000 range is shown in Fig. 3A_1. Each sub-oligosaccharide cluster comprised various *m/z* values that were $\Delta -(16 + n * 2)$, $\Delta -(30 + n * 2)$, $\Delta -(46 + n * 2)$, $\Delta -(62 + n * 2)$, and $\Delta -(78 + n * 2)$ Da relative to the corresponding DP-oligomer, where $n = 0$–4. The $n * 2$ present in each sub-oligosaccharide cluster can be due to variable levels (n) of dialdehydes (Fig. S6), as a dialdehyde sugar is 2 Da lower than an intact sugar unit.

The sub-oligosaccharide cluster with P_n $\Delta -(30 + n * 2)$ Da, with $n =$ 0, 1, and 2 (Fig. 3A_1) can be attributed to double oxidation of the terminal non-reducing end (NRE-) Xyl, as described in Scheme 1. At this Xyl unit, periodate will attack the three vicinal hydroxyl groups at C2, C3, and C4, releasing a molecule of formic acid from C3, and forming aldehyde groups at C2 and C4 positions (Halsall et al., 1947; Pereira et al., 2018; Perlin, 2006). The sub-oligosaccharide cluster with P_n $\Delta -(60 + n * 2)$ Da, with $n = 1$ and 2, can be attributed to the oxidation of the reducing end (RE-) Xyl unit. At this unit, oxidation can occur at C1—C2 and C2—C3 bonds, creating an aldehyde in the C3 position, whereas the C1—C2 bond is cleaved off as $C_2H_4O_2$ (glycolaldehyde; Scheme 1) (Hough et al., 1958; Pereira et al., 2018; Perlin, 2006). If a dialdehyde Xyl unit in the backbone undergoes intra-molecular cleavage at the C5—O—C1 linkage (Simões et al., 2016), an oligosaccharide containing a —O—CHOHCHO at the NRE-Xyl will be formed, which is (P_n −74) Da (Scheme 1). This intra-molecular cleavage combined with the presence of dialdehydes could explain the sub-oligosaccharide cluster with P_n $\Delta -(74 + n * 2)$ Da, with $n = 2$, 3 and 4. The other oligosaccharide generated from the intra-molecular cleavage will keep —O—$CHCH_2OHCHO$ at the RE-position, (P_n −60) Da. Thus, these results show that dialdehydes formation can be accompanied by cleavages within the oxidized sugar unit during oxidation.

For BWX, the pOx-BWX at RT for 6 h using a $NaIO_4$/PS ratio of 3.0 was chosen to be characterized by ESI-MS as it was about 40% oxidized (Fig. 2B), and it comprised many molecules within the DP 2–20 range (Fig. 1B). In the *m/z* 650–1000 range this pOx-BWX comprised P_n and clusters of oxidized oligosaccharides (Fig. 3B), confirming that this pOx-BWX was partially oxidized. Notably, the ESI-MS profile of pOx-BWX was different from pOx-AX (Fig. 3A_1), confirming that periodate oxidation of structurally different pentose-based polymers indeed generates polysaccharide structure-dependent oxidized oligosaccharides.

3.3.2. ESI-MS analysis of periodate-oxidized GM, XG, and HG samples

Regarding GM, XG, and HG, a high level of oligosaccharides was only obtained at 70 °C for 24 h using a $NaIO_4$/PS ratio of 6.0 for GM and XG, and a $NaIO_4$/PS ratio of 12.0 for HG (Fig. 1). The pOx-GM, pOx-XG and pOx-HG samples obtained under these periodate oxidations also mainly comprised clusters of oxidized oligosaccharides within the *m/z* 650–1000 range (ox-DP_n, Fig. 3C, D, and E). Especially for pOx-HG, still some non-oxidized oligomers were identified, which were composed of galacturonic acid units with and without methyl-esters (Fig. 3E).

As already described for pOx-AX, the oxidized oligosaccharide clusters observed for pOx-GM, pOx-XG, and pOx-HG in Fig. 3 could also derive from the three pathways described in Scheme 1, or even from a combination of it: (1) release of formic acid with formation of a

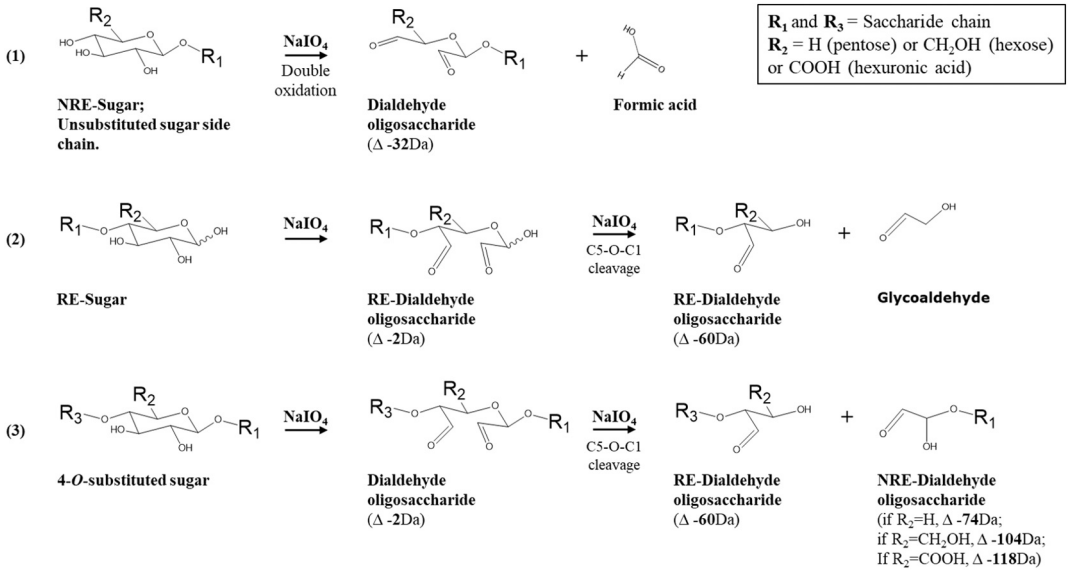

Scheme 1. Schematic fragmentations that a dialdehyde sugar unit of a polysaccharide can possibly undergo during periodate ($NaIO_4$) oxidation. NRE, non-reducing end; RE, reducing end. Δ −#Da, Da difference relative to the corresponding non-oxidized oligosaccharide with the same DP.

dialdehyde (Δ −32 Da) at the NRE-sugar units (Man for GM, Glc for XG, and GalA for HG) or at the unsubstituted sugar unit present in the side chain (Gal for GM and XG, and Xyl for XG); (2) oxidation of the RE-sugar with formation of an aldehyde at C3 position (Δ −60 Da) and release of C1 and C2 as $C_2H_4O_2$; and (3) intra-molecular cleavage of a dialdehyde sugar residue in the middle of the backbone (Man for GM, Glc for XG, and GalA for HG), resulting in two oligosaccharides. One of these oligosaccharides contains the terminal NRE-sugar and is Δ −60 Da relative to the respective non-oxidized DP-oligomer. The other oligosaccharide formed is Δ −104 Da versus the respective non-oxidized DP-oligomer of GM and XG, and Δ −118 Da relative to the respective non-oxidized and non-methyl-esterified DP-oligomer of HG.

When comparing all the ESI mass spectra (*m/z* 650–1000) in Fig. 3, it is seen that each sample had a unique MS oligosaccharide profile, being therefore PS structure-dependent. Thus, if a common condition based on periodate oxidation can be found among polysaccharides still generating

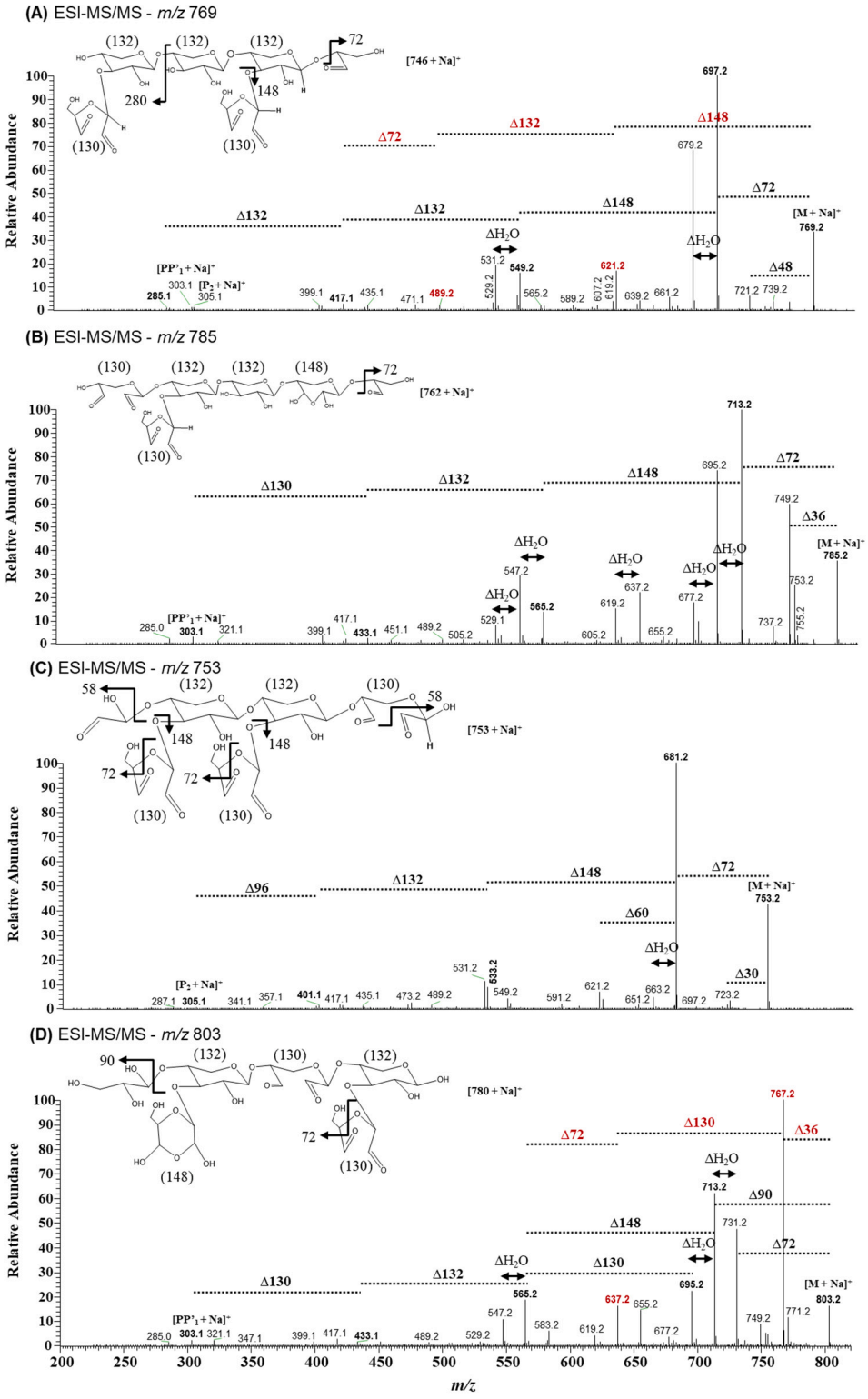

Fig. 4. ESI-MS/MS spectra of $[M + Na]^+$ ions *m/z* 769 (A), *m/z* 785 (B), *m/z* 753 (C), and *m/z* 803 (D) identified in Fig. 3 for pOx-AX. Potential ion structures and respective fragmentation pathways are depicted. $\mathbf{P_n}$ – oligomer with *n* pentoses; $\mathbf{P'_n}$ – oligomer with *n* dialdehyde pentoses. Number in parentheses (#) corresponds to the molecular weight of the dehydrated sugar form. Red numbers indicate a possible second fragmentation pathway. (For interpretation of the references to colour in this figure legend, the reader is referred to the web version of this article.)

the same MS oligosaccharide profiles, periodate oxidation of polysaccharides has good potential for polysaccharides fingerprinting by oligosaccharides.

3.4. ESI-MS/MS analysis of periodate-oxidized oligosaccharides

To reach a deeper understanding about the type of oxidized oligosaccharides observed in Fig. 3, and to study if their structures are solely due to the mechanisms proposed in Scheme 1, tandem MS (ESI-MS/MS) was performed on the most abundant oligosaccharides of each sub-oligosaccharide cluster present in the first **ox-DP$_n$**-cluster. The fragmentation patterns of the oxidized oligosaccharides obtained for pOx-AX will be discussed in detail below. As the oxidized oligosaccharides of pOx-BWX, pOx-GM, pOx-XG, and pOx-HG were found by MS/MS to be formed by the mechanisms proposed for pOx-AX, their fragmentation patterns will be briefly discussed and summarized.

3.4.1. Oligosaccharides from pOx-AX

Based on the fragmentation spectrum of the ion *m/z* 769 ($[M + Na]^+$, Fig. 4A) of pOx-AX, this ion was tentatively identified as an oligosaccharide with a DP 6 comprising three pentose (Xyl) units, two dialdehyde pentose (Ara) units, and a reducing end originating fragment comprising —O—CHCH$_2$OHCHO. This was deducted from the presence of fragment ions differing 132 Da (anhydro-pentose), 148 Da (dialdehyde pentose), and 72 Da (Fig. 4A). Considering that this pOx-AX was fully oxidized (Fig. 2A), the Δ 132 Da fragment most likely indicates the presence of a substituted Xyl unit. The Δ 72 Da fragment shows that the C1—C2 bond of a dialdehyde Xyl at the reducing end can be cleaved off as $C_2H_4O_2$ (Hough et al., 1958; Pereira et al., 2018; Perlin, 2006), and that this Xyl unit was unsubstituted. Similar fragmentation losses were observed for the parent ion *m/z* 785 ($[M + Na]^+$, Fig. 4B). This ion was tentatively identified as containing two pentose (Xyl) units, two dialdehyde pentoses (Xyl and Ara; 130 Da), one hemialdal pentose (Xyl; anhydro-hemialdal 148 Da) and a reducing end originating fragment

Table 2
Overview of the type of oxidized sugar units generated upon periodate oxidation of pOx-AX, pOx-BWX, pOx-GM, pOx-XG, and pOx-HG, as based on the ESI-MS/MS experiments.

	Oxidized sugar units identified				
Reaction type	pOx-AX	pOx-BWX	pOx-GM	pOx-XG	pOx-HG
Oxidation	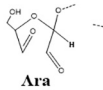 **Ara** **130**/148 **Xyl** **130**/148	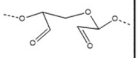 **Xyl** **130**/148	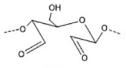 **Man** 160/178	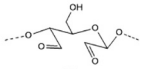 **Glc** **160**/178	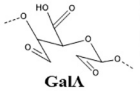 **GalA** **174**/192
Oxidation + Release of formic acid from C3					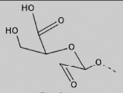 **GalA** 88/**106**
Double oxidation			 **Gal** **130**/148	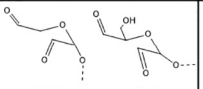 **Xyl** **100**/118 **Gal** **130**/148	
Hemialdal formation	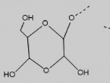 **Ara** **148**/166 **Xyl** **148**/166	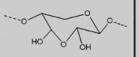 **Xyl** **148**/166	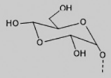 **Gal** **148**/166	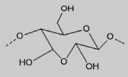 **Glc** 178/196	
Decarboxylation					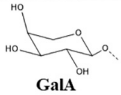 **GalA** **132**/150
Oxidation + -C5O–C1- cleavage	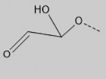 **Xyl** 58/76 **Xyl** **72**/90	 **Xyl** **72**/90	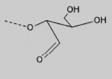 **Man** **102/120**	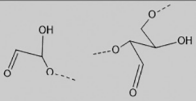 **Xyl** 58/76 **Glc** 102/120	
Hydrated aldehyde + -C5O–C1- cleavage				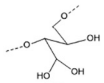 **Glc** 120/138	
Intra-molecular cleavage of a non-oxidized sugar unit	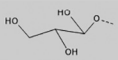 **Xyl** 72/**90**		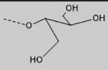 **Man** 104/122		

Name of the derived non-oxidized sugar unit is given below the depictured oxidized sugar unit. The molecular mass of the oxidized sugar unit in a non-hydrated and hydrated form (#-H$_2$O/#) is given under each structure, and the Δ *m/z* for this fragment observed in the ESI mass spectrum is highlighted in bold.

with —O—CHCH$_2$OHCHO (Δ 72 Da). The Δ 148 Da fragment should be derived from a hemialdal pentose instead of a pentose since no other isomer combinations fit *m/z* 785. Hemialdal structures upon periodate oxidation of other polysaccharides, such as GM and cellulose, have already been reported (da Silva et al., 2020; Nypelö et al., 2021; Sirviö et al., 2014).

The *m/z* 753 and 803 ions (Fig. 4) of pOx-AX were tentatively characterized as containing $C_2H_3O_2$ and $C_3H_5O_3$ at the non-reducing end, respectively, in addition to pentoses, dialdehyde pentoses, and hemialdal pentoses. The $C_2H_3O_2$ and $C_3H_5O_3$ remnants indicate intra-molecular cleavage of a dialdehyde pentose and of a non-oxidized pentose, respectively, which is indicative for the presence of an unsubstituted Xyl unit. To the best of our knowledge, the intra-molecular cleavage of a non-oxidized pentose, highlighted by the presence of a fragment ion with a Δ *m/z* 90 (Fig. 4D), has never been reported during periodate oxidation. Hence, these results indicate that besides

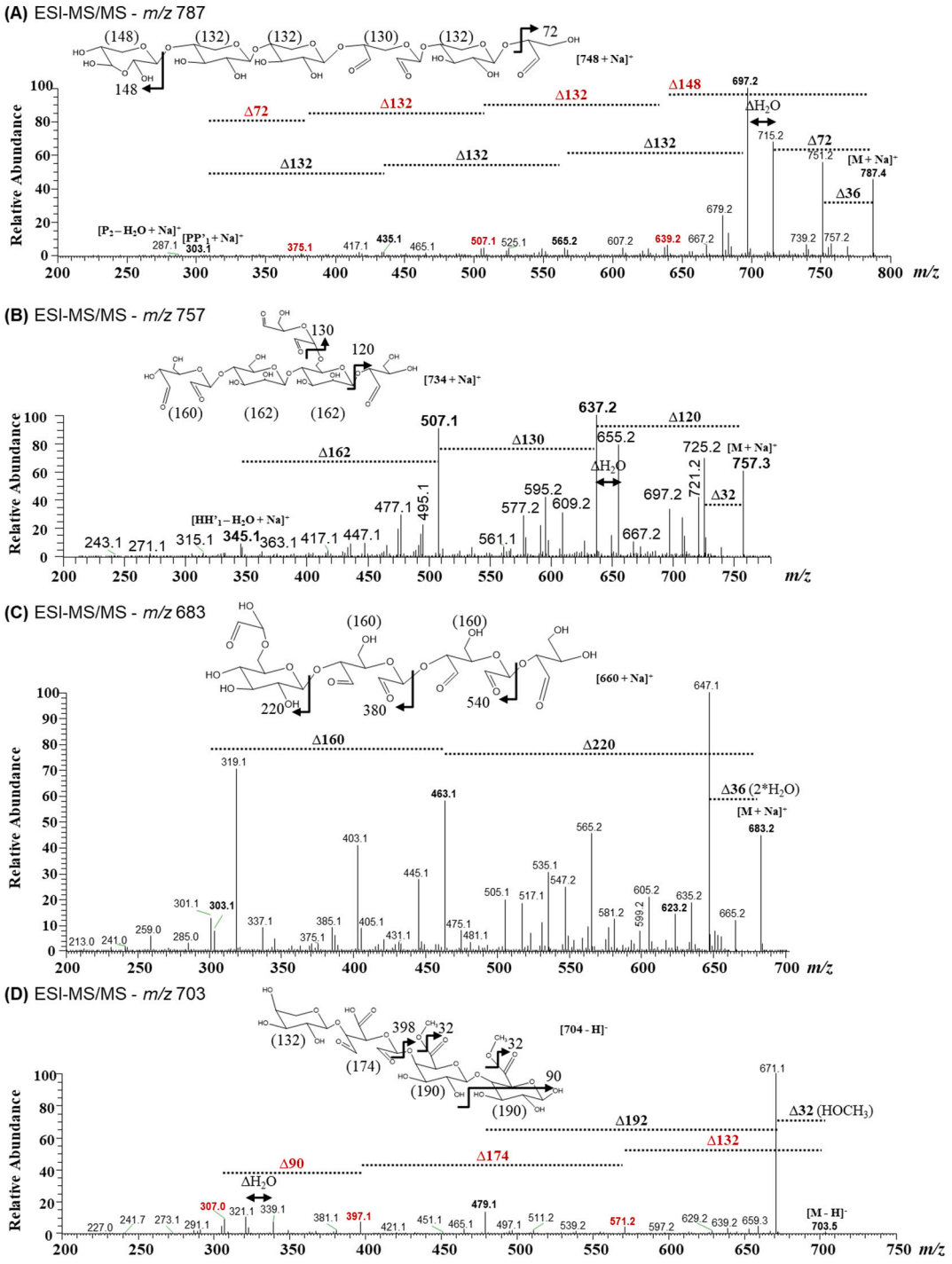

Fig. 5. ESI-MS/MS spectra of $[M + Na]^+$ ions *m/z* 787 (A), *m/z* 757 (B), and *m/z* 683 (C) identified in Fig. 3 for pOx-BWX, pOx-GM, and pOx-XG, respectively. ESI-MS/MS spectrum of the *m/z* 703 $[M-H]^-$ ion (D) identified in Fig. 3 for pOx-HG. Potential ion structures and respective fragmentation pathways are depicted. $\mathbf{P_n}$ or $\mathbf{H_n}$ – oligomer with n pentoses or hexoses; $\mathbf{P'_n}$ or $\mathbf{H'_n}$ – oligomer with n dialdehyde pentoses or hexoses. Number in parentheses (#) corresponds to the molecular weight of the dehydrated sugar form. Red numbers indicate a possible second fragmentation pathway. (For interpretation of the references to colour in this figure legend, the reader is referred to the web version of this article.)

dialdehyde formation (the mechanisms proposed in Scheme 1) and the formation of hemialdals (da Silva et al., 2020; Nypelö et al., 2021; Sirviö et al., 2014), periodate oxidation can be accompanied by intra-molecular cleavages of non-oxidized sugar units. The oxidized sugar components identified by ESI-MS/MS are summarized in Table 2.

Although tandem MS provided insights in the structure of the released oxidized oligosaccharides and allowed us to speculate about the composition of the native AX, detailed AX characterization is difficult to achieve. This is due to the high complexity of the oxidized oligosaccharides and the impossibility to distinguish isomers by ESI-MS via direct infusion, which hinders precise location of the substituents along the polymer backbone and/or of the (oxidized) sugar units.

3.4.2. Oligosaccharides from pOx-BWX, pOx-GM, pOx-XG, and pOx-HG

ESI-MS(/MS) analysis of the oxidized oligosaccharides of pOx-BWX, pOx-GM, pOx-XG, and pOx-HG samples allowed us to identify 1) dialdehyde sugar units; 2) double oxidized sugar units, 3) hemialdals; 4) oligosaccharides containing fragments originating from dialdehyde formation followed by cleavage of the C5—O—C1 bond at both reducing and/or non-reducing sugar ends; and 5) intra-molecular cleavages of non-oxidized sugar units. Additionally, decarboxylation of the sugar units was exclusively found for pOx-HG. A summary of these oxidized sugar components identified by ESI-MS/MS for each pOx-PS sample is shown in Table 2.

Fig. 5 illustrates the presence of these oligosaccharide oxidation products in the ESI-MS^2 spectra of the parental ions (m/z 787 of pOx-BWX, m/z 757 of pOx-GM, m/z 683 of pOx-XG, and m/z 703 of pOx-HG) that were present in the original spectra shown in Fig. 3. ESI-MS^2 spectra of the other major m/z values corresponding to oxidized oligosaccharides present in the first cluster of each sample in Fig. 3 are shown in Figs. S7, S8, S9 and S10.

The tentatively assigned structures for the ions m/z 757 (Fig. 5B) and 761 (Fig. S8) of pOx-GM, and for the m/z 683 of pOx-XG (Fig. 5C) had only one modified sugar unit side chain per four (oxidized) sugar moieties in the backbone. As mentioned before, precise positioning of the substituents along the backbone and of the oxidized units in the backbone is not possible due to the presence of isomers. Nevertheless, the tentatively assigned structures suggest that debranching of GM and XG occurred during periodate oxidation at 70 °C for 24 h using a $NaIO_4$/PS ratio of 6.0. This can be substantiated since guar GM has a Gal:Man ratio of ~1:2 and a structure with repeating blocks typical of [α-Gal(1→6)-β-Man(1→4)-β-Man(1→4)[α-Gal(1→6)]-β-Man(1→]$_n$ (Daas et al., 2000; Prajapati et al., 2013). XG is made up of repeating substituted backbone units composed of X-(L/)X-(L/)X-G (Mishra & Malhotra, 2009). Therefore, although the released oligosaccharides from GM and XG (70 °C, 24 h, $NaIO_4$/PS ratio of 6.0), and from HG (70 °C, 24 h, $NaIO_4$/PS ratio of 12.0) were not diagnostic due to partial debranching and removal of non-sugar substituents, unique MS profiles could be formed per PS sample (Fig. 3). Furthermore, these oligosaccharides were indicative of the type of the PS class, showing that periodate oxidation has potential to identify PS classes based on the oxidized oligosaccharide profiles.

4. Conclusions

In this study, we demonstrated that structurally different polysaccharides require different periodate oxidation conditions to be depolymerized to oligosaccharides. ESI-MS analyses showed characteristic oligosaccharide profiles, comprising polysaccharide (PS) structure-dependent oxidized oligosaccharide clusters. The oxidized oligosaccharide clusters had highly complex structures, comprising dialdehyde sugar units and other oxidized sugar structures, such as hemialdals and decarboxylated sugars. The high structural complexity of these oligosaccharides hampered detailed characterization of the native PS structure. In addition, especially for galactomannan, xyloglucan, and homogalacturonan, the released oligosaccharides suffered from partial debranching and removal of non-sugar substituents. Although detailed characterization of the native PS structure based on the oxidized oligosaccharides formed could not be achieved, the oligosaccharides are indicative for the native PS structure, as clearly PS structure-dependent oligosaccharides are formed. Our results are a good demonstration that MS analysis of oligosaccharides derived from periodate oxidation of polysaccharide could be an interesting chemical-induced polysaccharide depolymerization approach to reach a more generic recognition of polysaccharides via oligosaccharides fingerprinting than the commonly used enzymatic and/or (partial) acid hydrolysis approaches. A pitfall of the last two approaches when applied to polysaccharides is that isomeric oligosaccharide structures might be released, which cannot be distinguished by MS. This would result in identical MS oligosaccharide profiles between for example AX and BWX samples. This limitation could be overcome by our proposed approach. Thus, periodate oxidation could be an interesting reaction to be included as basis of a chemical-induced polysaccharide depolymerization method to reach a more generic recognition of polysaccharides by MS. A novel chemical-induced polysaccharide depolymerization based on periodate oxidation and thermal hydrolysis will be the subject of a follow-up paper.

CRediT authorship contribution statement

All authors contributed to this study. Carolina O. Pandeirada, Hans-Gerd Janssen, Yvonne Westphal, and Henk A. Schols contributed to the conception and design. Carolina O. Pandeirada developed the methodology and carried out the experiments, being helped by Max Achterweust. Carolina O. Pandeirada prepared the original draft. All authors were involved in critically reviewing all data and in writing the final manuscript. All authors read and approved the final manuscript to submission in Carbohydrate Polymers.

Declaration of competing interest

The authors declare that they have no known competing financial interests or personal relationships that could have appeared to influence the work reported in this paper.

Appendix A. Supplementary data

Supplementary data to this article can be found online at https://doi.org/10.1016/j.carbpol.2022.119540.

References

Abdel-Akher, M., Hamilton, J. K., Montgomery, R., & Smith, F. (1952). A new procedure for the determination of the fine structure of polysaccharides. *Journal of the American Chemical Society, 74*(19), 4970–4971. https://doi.org/10.1021/ja01139a526

Åman, P., & Bengtsson, S. (1991). Periodate oxidation and degradation studies on the major water-soluble arabinoxylan in rye grain. *Carbohydrate Polymers, 15*(4), 405–414. https://doi.org/10.1016/0144-8617(91)90090-Y

Aspinall, G. O., & Ross, K. M. (1963). The degradation of two periodate-oxidised arabinoxylans. *Journal of the Chemical Society (Resumed)*, 1676–1680.

Bauer, S. (2012). Mass spectrometry for characterizing plant cell wall polysaccharides. *Front. Plant Sci., 3*(45). https://doi.org/10.3389/fpls.2012.00045

Beaugrand, J., Chambat, G., Wong, V. W. K., Goubet, F., Rémond, C., Paës, G., Benamrouche, S., Debeire, P., O'Donohue, M., & Chabbert, B. (2004). Impact and efficiency of GH10 and GH11 thermostable endoxylanases on wheat bran and alkali-extractable arabinoxylans. *Carbohydrate Research, 339*(15), 2529–2540. https://doi.org/10.1016/j.carres.2004.08.012

Blumenkrantz, N., & Asboe-Hansen, G. (1973). New method for quantitative determination of uronic acids. *Analytical Biochemistry, 54*(2), 484–489. https://doi.org/10.1016/0003-2697(73)90377-1

Bobbitt, J. M. (1956). Periodate oxidation of carbohydrates. In M. L. Wolfrom, & R. S. Tipson (Eds.), *Advances in carbohydrate chemistry* (Vol. 11, pp. 1–41). Academic Press.

Chemin, M., Rakotovelo, A., Ham-Pichavant, F., Chollet, G., Da Silva Perez, D., Petit-Conil, M., Cramail, H., & Grelier, S. (2016). Periodate oxidation of 4-O-methylglucuronoxylans: Influence of the reaction conditions. *Carbohydrate Polymers, 142*, 45–50. https://doi.org/10.1016/j.carbpol.2016.01.025

Chetouani, A., Follain, N., Marais, S., Rihouey, C., Elkolli, M., Bounekhel, M., Benachour, D., & Le Cerf, D. (2017). Physicochemical properties and biological activities of novel blend films using oxidized pectin/chitosan. *International Journal of*

Biological Macromolecules, 97, 348–356. https://doi.org/10.1016/j.ijbiomac.2017.01.018

da Silva, L. M., Araújo, L. F. S., Alvez, R. C., Ono, L., Sá, D. A. T., da Cunha, P. L. R., Monteiro de Paula, R. C., & Maciel, J. S. (2020). Promising alternative gum: Extraction, characterization, and oxidation of the galactomannan of Cassia fistula. *International Journal of Biological Macromolecules, 165*, 436–444. https://doi.org/10.1016/j.ijbiomac.2020.09.164

Daas, P. J. H., Schols, H. A., & de Jongh, H. H. J. (2000). On the galactosyl distribution of commercial galactomannans. *Carbohydrate Research, 329*(3), 609–619. https://doi.org/10.1016/S0008-6215(00)00209-3

De Ruiter, G. A., Schols, H. A., Voragen, A. G. J., & Rombouts, F. M. (1992). Carbohydrate analysis of water-soluble uronic acid-containing polysaccharides with high-performance anion-exchange chromatography using methanolysis combined with TFA hydrolysis is superior to four other methods. *Analytical Biochemistry, 207*(1), 176–185. https://doi.org/10.1016/0003-2697(92)90520-H

De Souza, A. C., Rietkerk, T., Selin, C. G. M., & Lankhorst, P. P. (2013). A robust and universal NMR method for the compositional analysis of polysaccharides. *Carbohydrate Polymers, 95*(2), 657–663. https://doi.org/10.1016/j.carbpol.2013.02.036

Deckers, H. A., Olieman, C., Rombouts, F. M., & Pilnik, W. (1986). Calibration and application of high-performance size exclusion columns for molecular weight distribution of pectins. *Carbohydrate Polymers, 6*(5), 361–378. https://doi.org/10.1016/0144-8617(86)90026-3

Ding, W., Zhou, J., Zeng, Y., Wang, Y. N., & Shi, B. (2017). Preparation of oxidized sodium alginate with different molecular weights and its application for crosslinking collagen fiber. *Carbohydrate Polymers, 157*, 1650–1656. https://doi.org/10.1016/j.carbpol.2016.11.045

Gupta, B., Tummalapalli, M., Deopura, B. L., & Alam, M. S. (2013). Functionalization of pectin by periodate oxidation. *Carbohydrate Polymers, 98*(1), 1160–1165. https://doi.org/10.1016/j.carbpol.2013.06.069

Gupta, D. S., Jann, B., Bajpai, K. S., & Sharma, S. C. (1987). Structure of a galactomannan from Cassia alata seed. *Carbohydrate Research, 162*(2), 271–276. https://doi.org/10.1016/0008-6215(87)80222-7

Halsall, T. G., Hirst, E. L., & Jones, J. K. N. (1947). Oxidation of carbohydrates by the periodate ion. *Journal of the Chemical Society (Resumed), 1427–1432*. https://doi.org/10.1039/jr9470001427

Harris, P. J., & Smith, B. G. (2006). Plant cell walls and cell-wall polysaccharides: Structures, properties and uses in food products. *International Journal of Food Science and Technology, 41*(Suppl. 2), 129–143. https://doi.org/10.1111/j.1365-2621.2006.01470.x

Hough, L., Taylor, T. J., Thomas, G. H. S., & Woods, B. M. (1958). 239. The oxidation of monosaccharides by periodate with reference to the formation of intermediary esters. *Journal of the Chemical Society (Resumed)*, 1212–1217. https://doi.org/10.1039/JR9580001212

Huisman, M. M. H., Oosterveld, A., & Schols, H. A. (2004). Fast determination of the degree of methyl esterification of pectins by head-space GC. *Food Hydrocolloids, 18*(4), 665–668. https://doi.org/10.1016/j.foodhyd.2003.11.006

Izydorczyk, M. S., & Biliaderis, C. G. (1995). Cereal arabinoxylans: Advances in structure and physicochemical properties. *Carbohydrate Polymers, 28*(1), 33–48. https://doi.org/10.1016/0144-8617(95)00077-1

Jermendi, É., Beukema, M., van den Berg, M. A., de Vos, P., & Schols, H. A. (2022). Revealing methyl-esterification patterns of pectins by enzymatic fingerprinting: Beyond the degree of blockiness. *Carbohydrate Polymers, 277*. https://doi.org/10.1016/j.carbpol.2021.118813

Kholiya, F., Chaudhary, J. P., Vadodariya, N., & Meena, R. (2016). Synthesis of bio-based aldehyde from seaweed polysaccharide and its interaction with bovine serum albumin. *Carbohydrate Polymers, 150*, 278–285. https://doi.org/10.1016/j.carbpol.2016.05.022

Kochumalayil, J. J., Morimune, S., Nishino, T., Ikkala, O., Walther, A., & Berglund, L. A. (2013a). Nacre-mimetic clay/xyloglucan bionanocomposites: A chemical modification route for hygromechanical performance at high humidity. *Biomacromolecules, 14*(11), 3842–3849. https://doi.org/10.1021/bm400883e

Kochumalayil, J. J., Zhou, Q., Kasai, W., & Berglund, L. A. (2013b). Regioselective modification of a xyloglucan hemicellulose for high-performance biopolymer barrier films. *Carbohydrate Polymers, 93*(2), 466–472. https://doi.org/10.1016/j.carbpol.2012.12.041

Kristiansen, K. A., Potthast, A., & Christensen, B. E. (2010). Periodate oxidation of polysaccharides for modification of chemical and physical properties. *Carbohydrate Research, 345*(10), 1264–1271. https://doi.org/10.1016/j.carres.2010.02.011

Lombard, V., Golaconda Ramulu, H., Drula, E., Coutinho, P. M., & Henrissat, B. (2014). The carbohydrate-active enzymes database (CAZy) in 2013. *Nucleic Acids Research, 42*(D1), D490–D495. https://doi.org/10.1093/nar/gkt1178

Majee, S. K., Bera, K., Raja, W., Ghosh, K., Ray, S., & Ray, B. (2016). Structural highlights of an antioxidative arabinogalactan protein of Lannea grandis gum that stabilizes β-lactoglobulin. *Food Hydrocolloids, 61*, 720–729. https://doi.org/10.1016/j.foodhyd.2016.06.016

Mishra, A., & Malhotra, A. V. (2009). Tamarind xyloglucan: A polysaccharide with versatile application potential. *Journal of Materials Chemistry, 19*(45), 8528–8536. https://doi.org/10.1039/b911150f

Morelle, W., Lemoine, J., & Strecker, G. (1998). Structural analysis of O-linked oligosaccharide-alditols by electrospray-tandem mass spectrometry after mild periodate oxidation and derivatization with 2-aminopyridine. *Analytical Biochemistry, 259*(1), 16–27. https://doi.org/10.1006/abio.1998.2618

Nypelö, T., Berke, B., Spirk, S., & Sirviö, J. A. (2021). Review: Periodate oxidation of wood polysaccharides—Modulation of hierarchies. *Carbohydrate Polymers, 252*. https://doi.org/10.1016/j.carbpol.2020.117105

Pandeirada, C. O., Merkx, D. W. H., Janssen, H.-G., Westphal, Y., & Schols, H. A. (2021). TEMPO/NaClO2/NaOCl oxidation of arabinoxylans. *Carbohydrate Polymers, 259*, Article 117781. https://doi.org/10.1016/j.carbpol.2021.117781

Pereira, I., Simões, J., Evtyugin, D. V., Rouif, S., Coimbra, M. A., Domingues, M. R. M., & Gama, M. (2018). Effects of gamma irradiation and periodate oxidation on the structure of dextrin assessed by mass spectrometry. *European Polymer Journal, 103*, 158–169. https://doi.org/10.1016/j.eurpolymj.2018.04.011

Perlin, A. S. (2006). Glycol-cleavage oxidation. *Advances in Carbohydrate Chemistry and Biochemistry, 60*, 183–250. https://doi.org/10.1016/S0065-2318(06)60005-X

Peterson, G. (1974). Gas-chromatographic analysis of sugars and related hydroxy acids as acyclic oxime and ester trimethylsilyl derivatives. *Carbohydrate Research, 33*(1), 47–61. https://doi.org/10.1016/S0008-6215(00)82939-0

Prajapati, V. D., Jani, G. K., Moradiya, N. G., Randeria, N. P., Nagar, B. J., Naikwadi, N. N., & Variya, B. C. (2013). Galactomannan: A versatile biodegradable seed polysaccharide. *International Journal of Biological Macromolecules, 60*, 83–92. https://doi.org/10.1016/j.ijbiomac.2013.05.017

Ruiz-Matute, A. I., Hernández-Hernández, O., Rodríguez-Sánchez, S., Sanz, M. L., & Martínez-Castro, I. (2011). Derivatization of carbohydrates for GC and GC-MS analyses. *Journal of Chromatography B: Analytical Technologies in the Biomedical and Life Sciences, 879*(17–18), 1226–1240. https://doi.org/10.1016/j.jchromb.2010.11.013

Saha, A., Tyagi, S., Gupta, R. K., & Tyagi, Y. K. (2017). Natural gums of plant origin as edible coatings for food industry applications. *Critical Reviews in Biotechnology, 37*(8), 959–973. https://doi.org/10.1080/07388551.2017.1286449

Simas-Tosin, F. F., de Souza, L. M., Wagner, R., Pereira, G. C. Z., Barraza, R. R., Wendel, C. F., Sassaki, G. L., Iacomini, M., & Gorin, P. A. J. (2013). Structural characterization of a glucuronoarabinoxylan from pineapple (Ananas comosus (L.) Merrill) gum exudate. *Carbohydrate Polymers, 94*(1), 704–711. https://doi.org/10.1016/j.carbpol.2012.12.059

Simões, J., Moreira, A. S. P., da Costa, E., Evtyugin, D., Domingues, P., Nunes, F. M., Coimbra, M. A., & Domingues, M. R. M. (2016). Oxidation of amylose and amylopectin by hydroxyl radicals assessed by electrospray ionisation mass spectrometry. *Carbohydrate Polymers, 148*, 290–299. https://doi.org/10.1016/j.carbpol.2016.03.034

Sims, I. M., Carnachan, S. M., Bell, T. J., & Hinkley, S. F. R. (2018). Methylation analysis of polysaccharides: Technical advice. *Carbohydrate Polymers, 188*, 1–7. https://doi.org/10.1016/j.carbpol.2017.12.075

Sirvio, J., Hyvakko, U., Liimatainen, H., Niinimaki, J., & Hormi, O. (2011). Periodate oxidation of cellulose at elevated temperatures using metal salts as cellulose activators. *Carbohydrate Polymers, 83*(3), 1293–1297. https://doi.org/10.1016/j.carbpol.2010.09.036

Sirviö, J. A., Liimatainen, H., Visanko, M., & Niinimäki, J. (2014). Optimization of dicarboxylic acid cellulose synthesis: Reaction stoichiometry and role of hypochlorite scavengers. *Carbohydrate Polymers, 114*, 73–77. https://doi.org/10.1016/j.carbpol.2014.07.081

Spedding, H. (1960). 628. Infrared spectra of periodate-oxidised cellulose. *Journal of the Chemical Society (Resumed)*, 3147–3152. https://doi.org/10.1039/jr9600003147

Thibault, J., & JF, T. (1979). *Automatisation du dosage des substances pectiques par la méthode au métahydroxydiphényl*.

Westphal, Y., Schols, H. A., Voragen, A. G. J., & Gruppen, H. (2010). MALDI-TOF MS and CE-LIF fingerprinting of plant cell wall polysaccharide digests as a screening tool for arabidopsis cell wall mutants. *Journal of Agricultural and Food Chemistry, 58*(8), 4644–4652. https://doi.org/10.1021/jf100283b

Willför, S., Pranovich, A., Tamminen, T., Puls, J., Laine, C., Suurnäkki, A., Saake, B., Uotila, K., Simolin, H., Hemming, J., & Holmbom, B. (2009). Carbohydrate analysis of plant materials with uronic acid-containing polysaccharides–A comparison between different hydrolysis and subsequent chromatographic analytical techniques. *Industrial Crops and Products, 29*(2), 571–580. https://doi.org/10.1016/j.indcrop.2008.11.003